Title: Influence of mechanical damage induced in laboratory on the soil-geosynthetic interaction in inclined-plane shear

Authors: M. Pinho-Lopes[*1] and M.L. Lopes[2]

[1] Lecturer, Faculty of Engineering and the Environment, University of Southampton, Highfield, Southampton SO17 1BJ, United Kingdom, Telephone: +44 (0)2380598363; Fax: +442380677519; Email: M.Pinho-Lopes@soton.ac.uk

[2] Full Professor, CONSTRUCT-GEO, Department of Civil Engineering, Faculty of Engineering, University of Porto, Rua Dr. Roberto Frias, s/n 4200-465 Porto Portugal, Telephone: +3515081564; Fax: +3515081446; E-mail: lcosta@fe.up.pt

[*] Corresponding author

Declarations of interest: none

Abstract:

This paper contributes to better understanding how mechanical damage associated with installation affects soil-geosynthetic interaction, particularly for inclined plane shear movement. The mechanical damage was induced in laboratory, adapting a standardised procedure to allow for large samples. Six geosynthetics were studied: two geotextiles, one geocomposite and three geogrids. The soil-geosynthetic interface was characterised using inclined plane shear tests. The laboratory mechanical damage affected the soil-geosynthetic interface strength and the sliding mechanisms observed. The results showed that the mechanical damage caused an increase in the skin friction available, due to the damage mechanisms observed. The structure of the geosynthetic affected the inclined plane shear response after mechanical damage. The friction mobilised in solid area of the geogrids increased after mechanical damage, which depended on the geogrid and on the consequences of mechanical damage. The reduction factors for mechanical damage associated to installation

showed that the interface strength did not change significantly. The reduction factor obtained from tensile tests was, in most cases, conservative to represent the changes observed on the soil-geosynthetic interface strength. The structure of the geosynthetics had a higher impact on their tensile response after mechanical damage than on the soil-geosynthetic interface in inclined plane shear. For the interface strength in inclined shear plane movement, the mechanical damage induced in laboratory of the woven geotextile was conservative compared to field installation damage, while for the woven geogrid the mechanical damage induced in laboratory was within the range of damage induced in the field. Despite some heterogeneity of responses, the standardised laboratory tests to induce mechanical damage in laboratory seem to be able to represent the effect of the mechanical damage associated with installation on the inclined plane shear response of soil-geosynthetic interfaces.

Keywords:

Geosynthetics, mechanical damage, coefficient of interaction, inclined plane shear, reduction factor

1 INTRODUCTION

Mechanical damage associated with installation is one of the key durability agents affecting the performance of geosynthetics. Particularly for applications in soil reinforcement, it is common to assess changes in tensile strength of the geosynthetics. However, the soil-geosynthetic interaction is essential for an effective development of the reinforcement mechanisms. Thus, it is important to understand if and how mechanical damage associated with installation influences the soil-geosynthetic interface strength. As inducing installation damage under real conditions is lengthy and expensive, laboratory simulations of that damage may be of use.

In this paper the influence of mechanical damage (associated with installation and induced in laboratory under standardised conditions) on the soil-geosynthetic interface strength in inclined plane shear movement was studied for one soil and six geosynthetics. The soil-geosynthetic interface strength and the sliding mechanisms developing were analysed. For two of the geosynthetics the influence of mechanical damage induced in laboratory on the inclined plane shear response was compared to installation damage induced in field under real conditions.

2 BACKGROUND

An effective transference of tensile stresses from soil to reinforcements is key for achieving reinforced soil structures with adequate performance. Thus, the soil-geosynthetic interface mechanisms and properties play a fundamental role in the design of reinforced soil structures. The inclined plane shear test is often used to characterise the soil-geosynthetic interaction under low normal pressures corresponding to soil heights above the geosynthetic up to 1.0 m, namely for slopes, such as linings in cover systems of waste disposal areas or erosion control systems (Palmeira et al. [1]).

The inclined plane shear test is a standardised procedure [2], which allows determining the angle of friction for the soil-geosynthetic interface by measuring the angle at which a box filled with soil slides when the base supporting the geosynthetic is inclined at a constant rate. This test procedure and its conventional interpretation have been criticised, as they do not capture differences in response commonly observed for both soil-geosynthetic and geosynthetic-geosynthetic interfaces and are non-conservative [3,4]. Additionally, the standardised inclined plane shear test procedure has been criticised because of the way the tests results are interpreted [3,4] but also because of the inclination rate used in the test. According to Briançon [5](2001), the inclination rate of (3.0±0.5) °/min prescribed in the inclined plane

shear test standardised procedure [2] influences the responses observed in the tests and recommended a smaller inclination rate (0.5±0.2) °/min. Nevertheless, according to Reyes Ramirez and Gourc [3], the inclination rate has no significant influence of inclined plane shear test results.

According to Gourc and Reyes Ramirez [4], the standard approach [2] for determining the soil-geosynthetic interface friction angle for a displacement of the upper box of 50 mm, ϕ_{50}^{stat}, uses a static analysis for a dynamic conditions. Gourc and Reyes Ramirez [4] identified three phases for the sliding behaviour of the upper box (Figure 1): phase 1, static; phase 2, transitory; phase 3, non-stabilised sliding. During phase 1 there is practically no movement of the upper box (displacement d=0), up to $\beta=\beta_0$. In phase 2 the upper box moves gradually downward with an increased acceleration, for increasing inclination ($\beta>\beta_0$) of the test equipment. Lastly, during phase 3 the upper box undergoes non-stabilised sliding at an increasing speed, even for a constant inclination angle ($\beta=\beta_s$) and constant acceleration. Two different sliding mechanisms can occur during the transitory phase [4]: i) sudden sliding, which is an abrupt displacement of the upper box (Figure 1a); ii) gradual sliding (displacement of the upper box increasing with the inclination). For the latter, a progressive or a stick-slip displacement can be observed (Figure 1b). According to Pitanga et al. [6], although for different conditions and kinematics, a gradual sliding in an inclined plane shear test can be related to a strain hardening response in direct shear, while the sudden sliding in inclined plane shear movement can be compared to strain softening behaviour under direct shear conditions. Gourc and Reyes Ramirez [4], reporting results for geosynthetic-geosynthetic interface, concluded that the sliding mechanism is not a characteristic response of those interfaces and depends on the load applied initially at the interface and on the surface of the geosynthetic.

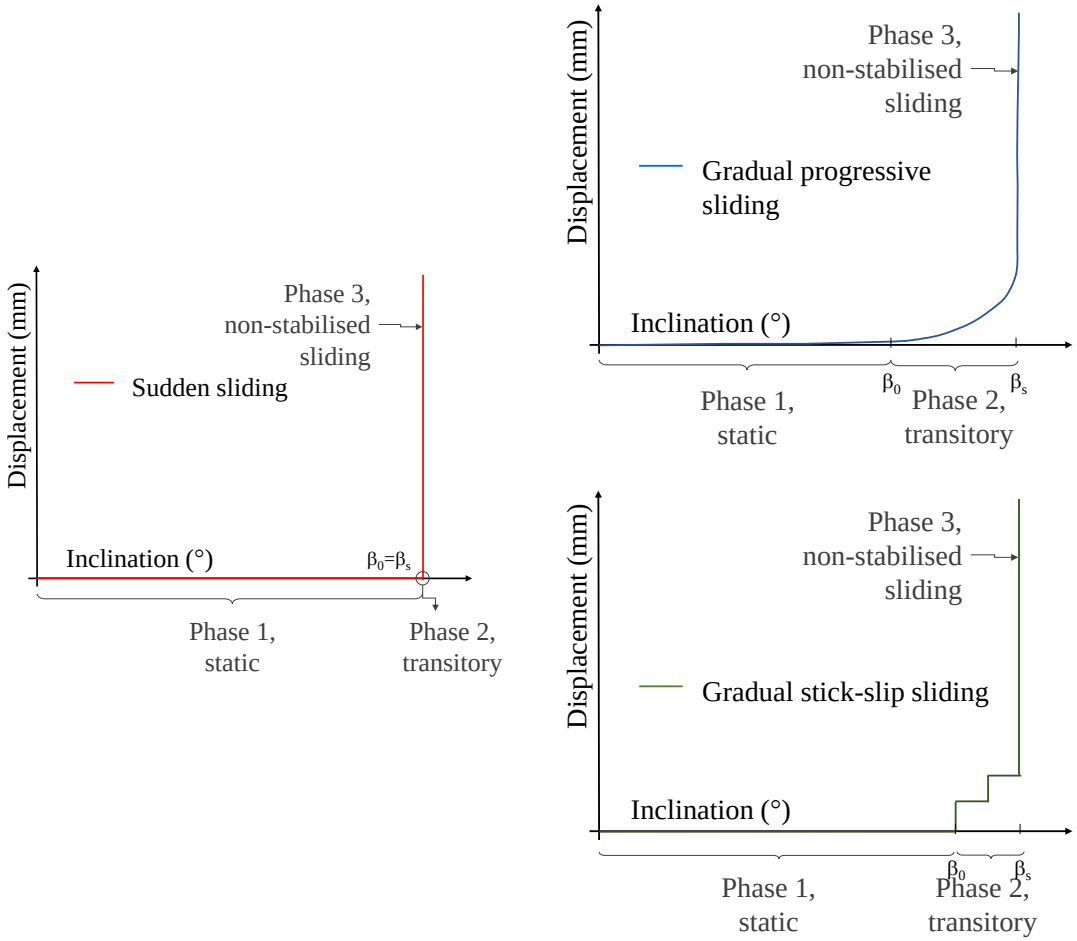

a) **b)**

Figure 1 – Schematic representation of the different sliding mechanisms typically observed in inclined plane shear tests with indication of the different sliding stages: a) sudden and b) gradual sliding (progressive and stick-slip) of the upper box.

Gourc and Reyes Ramirez [4] proposed an alternative static-dynamic interpretation of the inclined plane shear test which included two parameters: the initial friction angle, ϕ_0 , for static conditions (in particular, for the beginning of movement at static conditions); and the limit friction angle, ϕ_{lim}, measured during the uniformly accelerated movement occurring for the dynamic sliding. The static or initial friction angle, ϕ_0 (Equation 1) can be defined for a displacement of the upper box d=1 mm, representative of a small relative displacement [6]. The limit friction angle for constant acceleration, $\gamma = \gamma_c$, ϕ_{lim} can be obtained from Equation 2;

the standard friction angle, ϕ_{50}^{stat} (Equation 3) is identified as pseudo-static, because the actual conditions are not static [6].

$$\tan \phi_0 = \frac{(m_b + m_s) \cdot g \cdot \sin \beta_0 - T_{guide}}{m_s \cdot g \cdot \cos \beta_0} \quad (1)$$

$$\tan \phi_{\lim} = \frac{(m_b + m_s) \cdot g \cdot \sin \beta_{\lim} - T_{guide} - (m_b + m_s) \cdot \gamma_c}{m_s \cdot g \cdot \cos \beta_{\lim}} \quad (2)$$

$$\tan \phi_{50}^{stat} = \frac{(m_b + m_s) \cdot g \cdot \sin \beta_{50} - T_{guide}}{m_s \cdot g \cdot \cos \beta_{50}} \quad (3)$$

Where m_b is the mass of the upper box, m_s is the mass of soil in the upper box, g is the acceleration of gravity, T_{guide} is the tangential component of the reaction of the guidance system, β_0 is the inclination at the end of phase 1, β_{lim} is the inclination for constant acceleration (γ_c), and β_{50} is the inclination for a displacement of the upper box of 50 mm.

For soil-geosynthetic interfaces, a sudden failure may be expected, as the start of the sliding induces a loosening of the soil packing; thus, according to Gourc and Reyes Ramirez [4], the friction angles ϕ_0 and ϕ_{lim} are close to the peak and residual values for the angle of friction estimated in a shear box, except for the dynamic effect on the packing. According to Briançon et al. [7], the standard method EN ISO 12957-2 [1] overestimates the friction angle of several geosynthetic-geosynthetic interfaces, in particular for gradual sliding. Such conclusions were based on an alternative inclined plane shear method (designated as a "force procedure") proposed by Briançon et al. [7], which requires significant modifications of test equipment developed according to EN ISO 12957-2 [1].

When reinforced structures are built, the geosynthetic reinforcements are submitted to mechanical loading that can cause damage and, in some cases, compromise their ability to perform their functions adequately. In the literature, several studies can be found on how installation damage can affect the tensile response of geosynthetics, for the short-term [8-12] and long-term responses [13-18]. However, there is limited information on how installation

damage can influence the soil-geosynthetic interaction. To address that, Pinho-Lopes et al. [19] studied the effect of installation damage under real conditions on the strength of soil-geogrids interface during pullout and Pinho-Lopes et al. [20] compared the influence of installation damage induced in full scale test banks on the soil-geosynthetic interface strength in both pullout and inclined plane shear. According to Pinho-Lopes et al. [20], the compaction processes can cause the accumulation of a layer of fine particles over the geosynthetics, which for fine backfill materials can very important; this thus leads to a reduction in available skin friction at the soil-geosynthetic interface. Pinho-Lopes et al. [20] concluded that, for the woven geotextile and woven geogrid studied, the soil-geosynthetic coefficient of interaction in inclined plane shear was little influenced by the field installation damage induced; the accumulation of fines on the geosynthetic surface caused most of the changes observed. Additionally, the authors [20] found that the effects of the installation conditions on the soil–geosynthetic interface, regardless of the type of movement analysed (pullout or inclined plane shear), were overestimated when using a similar reduction factor obtained from tensile tests. To complement the results reported by Pinho-Lopes et al. [20], more tests, including a variety of installation conditions and geosynthetics would be necessary. Nonetheless, inducing field installation damage under real conditions is quite expensive and time consuming. Thus, the use of laboratory simulations to replicate such damage or its effects should be investigated.

Therefore, in this paper the soil-geosynthetic interaction response of six geosynthetics was studied using inclined-plane shear tests, to better understand the changes in response after mechanical damage associated with installation induced in laboratory and under standardised conditions. Reduction factors for mechanical damage were calculated, to contribute to the creation of databases for the design of reinforced soil structures.

3 EXPERIMENTAL PROGRAM

3.1 Geosynthetics

Six geosynthetics were studied (Table 1 and Figure 2):

- a woven geotextile (GTXw), consisting of polypropylene (PP) tapes;
- a nonwoven geotextile (GTXn) consisting of continuous mechanically bonded polypropylene (PP) filaments;
- an uniaxial geocomposite (GCR) constituted by high modulus polyester (PET) fibres (yarns) attached to a nonwoven continuous filament PP geotextile backing;
- a woven geogrid (GGRw), comprising high modulus PET fibres knitted in a flat orientation and covered with a protective polymeric coating;
- a PP extruded biaxial geogrid (GGRb);
- a high density polyethylene (HDPE) extruded uniaxial geogrid (GGRu).

The geosynthetics were chosen to include materials with similar nominal tensile strength and different structures (group 1, GTXn, GCR, GGRw; group 2, GTXw, GGRu) and with similar structure and different nominal tensile strength and manufacturing process (for example, the three different geogrids analysed, GGRw, GGRb, GGRu).

Table 1 – Characteristics of the geosynthetics tested.

Property	Geosynthetic					
	GTXw	GTXn	GCR	GGRw	GGRb	GGRu
Polymer	PP	PP	PET/PP	PET	PP	HDPE
Mass per unit area, μ (g/m^2)	320	1000	321	380	530	450
Nominal thickness, d_{2kPa} (mm)	1.2	7.2	2.1	1.7	-	-
Thickness of longitudinal ribs, d_{long} (mm)	-	-	-	1.6	2.2	1.1
Thickness of transverse ribs, d_{trans} (mm)	-	-	-	1.6	1.4	2.7
Mean grid openings dimensions (mm x mm)	-	-	-	25×25	33×33	22×235

Short-term tensile strength (kN/m)	65	55	58	58	40	68
Strain at maximum load (%)	11.0	105.0	10.0	10.5	11.0	9.0

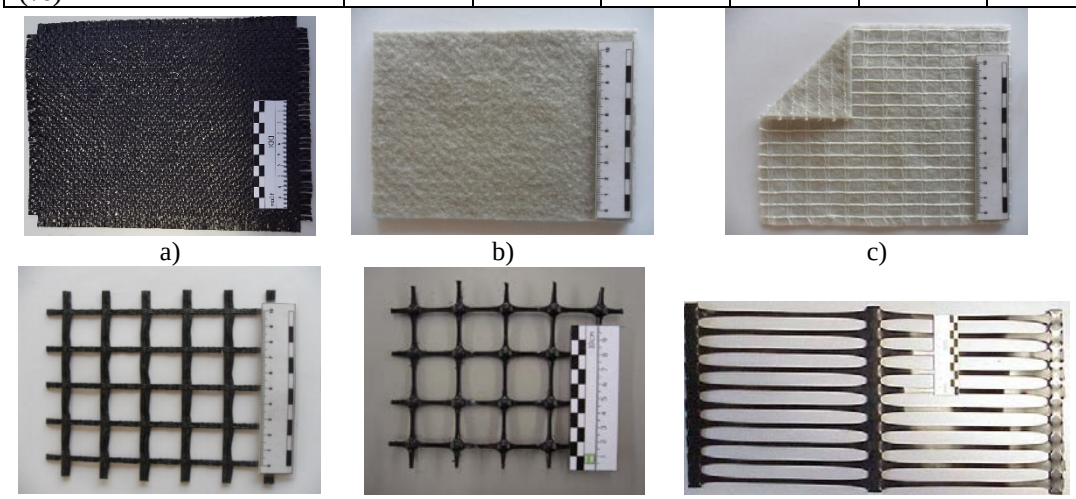

Figure 2 – Geosynthetics studied: a) GTXw; b) GTXn; c) GCR; d) GGRw; e) GGRb; f) GGRu.

3.2 Test program

The test program presented in this paper included two groups of tests: 1) laboratory mechanical damage of the geosynthetics; 2) characterisation of the soil-geosynthetic interface of the undamaged and the damaged geosynthetics using inclined-plane shear tests (Table 2).

Table 2 - Test program implemented and number of specimens tested.

Geosynthetic	Sample	Mechanical damage (Adapted from EN ISO 10722 [21])	Inclined plane shear (EN ISO 12957-2 [2])
GTXw	UND	–	3
	LAB D	3	3
GTXn	UND	–	3
	LAB D	3	3
GCR	UND	–	3
	LAB D	3	3
GGRw	UND	–	3
	LAB D	3	3
GGRb	UND	–	3
	LAB D	3	3
GGRu	UND	–	3

	LAB D	3	3

GTXw – woven geotextile | GTXn – nonwoven geotextile | GCR – reinforcement geocomposite

GGRw – woven geogrid | GGRb – biaxial extruded geogrid | GGRu – uniaxial extruded geogrid

UND – undamaged | LAB D – submitted to mechanical damage in laboratory

3.2.1 Laboratory mechanical damage test

Currently there is a standardised procedure to induce mechanical damage of geosynthetics in laboratory EN ISO 10722 [21]. That procedure includes confining a geosynthetic specimen between layers of a synthetic aggregate; the material is then submitted to cyclic loading. The synthetic aggregate is a sintered aluminium oxide (also known as corundum) with particle sizes ranging between 5 mm and 10 mm. To ensure the aggregate maintains its characteristics during the tests, the standardised procedure followed recommends that, if necessary, after every three uses the aggregate is wet sieved (using a 5 mm aperture sieve), to eliminate particles smaller than 5 mm. Additionally, after 20 uses the aggregate should be completely discarded. The test container is formed by two half-boxes. The lower half-box is filled with two consecutive layers of compacted aggregate (0.75 m high in total). The compaction is achieved applying a static pressure of 200 kPa for 1 minute with a plate with the same plane area as the container. The geosynthetic is placed on top of the lower half-box; the upper part of the container is then filled with loose aggregate (0.75 m high). The loading plate is positioned on top of the loose aggregate and a cyclic loading ranging between 5 kPa and 500 kPa is applied, with frequency of 1 Hz for 200 cycles.

The standardised laboratory mechanical damage test was developed for testing small specimens of geosynthetics, with dimensions adequate for wide-width tensile tests (with a specimen area between clamps of 0.1 m in height and 0.2 m in width) or hydraulic tests (with comparable specimen dimensions). In the standard procedure (EN ISO 10722 [21]), the plan section of the loading plate has the same dimensions as the tensile test specimens between

clamps (0.1 x 0.2 m^2). As the specimens in the inclined plane shear tests are larger than that, it was necessary to adapt the damage test procedure and equipment to enable damaging large enough specimens under conditions similar to those in EN ISO 10722 [21]. For that, the original height of the container (EN ISO 10722 [21]) was kept and its plan section was enlarged. The dimensions of the loading plate were defined as those of the inclined plane shear specimens. The new load plate was 0.7 x 0.43 m^2 (the same as the larger specimens for the inclined plane shear test equipment used); the test box plan dimensions were defined using the same additional length and width relatively to the load plate as in the original test procedure (EN ISO 10722 [21]). A hydraulic system was used to apply the cyclic loading (Figure 3); these tests were performed in the Department of Civil Engineering, University of Aveiro, Portugal. Due to limitations of the test equipment, a frequency of 0.5 Hz was used (instead of 1 Hz), thus, the damage induced is more conservative that in EN ISO 10722 [21].

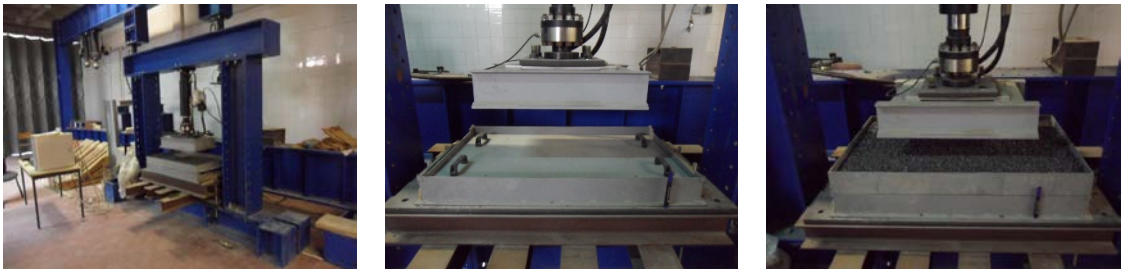

a) b) c)

Figure 3 – Laboratory mechanical damage tests: a) overview of the equipment; b) compaction of the first layer of aggregate; c) container ready for testing.

3.2.2 Inclined plane shear test

In the inclined plane shear tests the angle of friction for the soil-geosynthetic interface is quantified by determining the angle at which a box filled with soil slides when the base supporting the geosynthetic is inclined at a constant rate (EN ISO 12957-2 [2]). Depending on the type of geosynthetic, the specimen is supported on a rigid metal base (for sheet materials) or on a lower box filled with soil (for geogrids). The upper box includes two wedges with

inclination 1(H):2(V) placed in both the frontal and back walls of the box. The wedges ensure that the normal force applied passes through the centre of gravity of the upper box and that the distribution of normal stresses is uniform [1]. Additionally, to allow adjusting the height between the base of the upper box and the geosynthetic specimen and thus, preventing the self-weight of the upper box to load the specimen, the upper box is supported on runners set laterally. Figure 4 illustrates the equipment used for the tests reported herein (more details can be found in [22]).

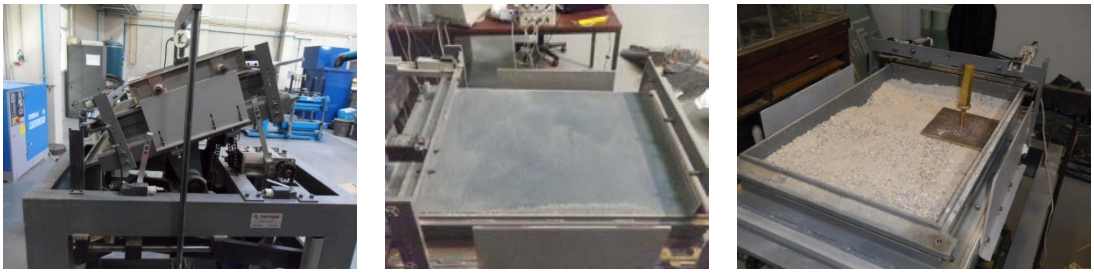

a) b) c)

Figure 4 – Inclined plane shear test equipment: a) during a test (upper box and geosynthetic supported on a rigid base); b) rigid base; c) lower box being filled with soil.

The geosynthetic specimens were 0.43 m wide and 0.70 m long when supported on a rigid base and 0.36 m wide and 0.60 m long when fixed on a lower box with soil. The specimens were tested under a vertical stress of 10 kPa and an inclination rate of 0.5 °/min, to address limitations identified by Briançon [5], while the inclination rate prescribed on EN ISO 12957-2 [2] is (3.0±0.5) °/min. For each sample, three specimens were tested. GTXw, GTXn and GCR were supported on the rigid base, while the geogrids studied (GGRw, GGRb and GGRu) were fixed on a lower box with soil.

The main properties of the soil used in contact with the geosynthetics are summarised in Table 3 and the particle size distribution is illustrated in Figure 5. In the inclined shear plane tests the soil was compacted to a relative density, I_D, of 50% to minimise any additional damage

during the test set-up, particularly due to spreading, levelling and compacting the soil. The shear strength of the soil was characterised for the same relative density using a large direct shear box.

Table 3 – Properties of the soil used in the inclined plane shear tests.

% Fines (<0.074mm) (%)	D_{10} (mm)	D_{50} (mm)	D_{max} (mm)	$\gamma^{\#}$ (kN/m^3)	$\phi'^{\#}$ (º)	$c'^{\#}$ (º)
3.63	0.19	2.67	10.00	17.61	42.5	8.49

$^{\#}$ for a relative density I_D=50%

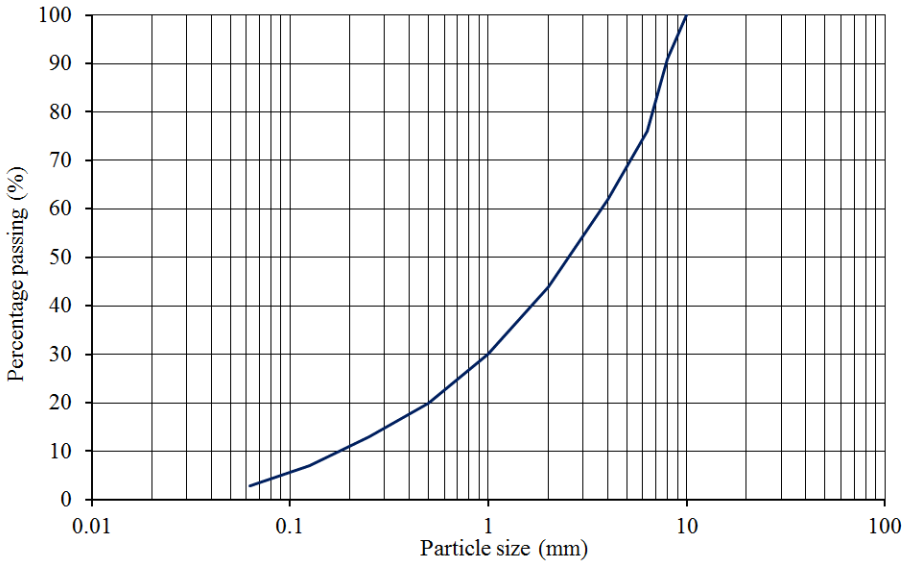

Figure 5. Particle size distribution of the soil used in the inclined plane shear tests.

4 RESULTS AND DISCUSSION

4.1 Mechanical damage observed

After the mechanical damage tests in laboratory, the specimens were examined visually to assess the impact of the mechanical damage induced. Figure 6 illustrates some typical consequences of the laboratory mechanical damage and Table 4 summarises the most common consequences of the mechanical damage induced observed for the six geosynthetics studied.

257

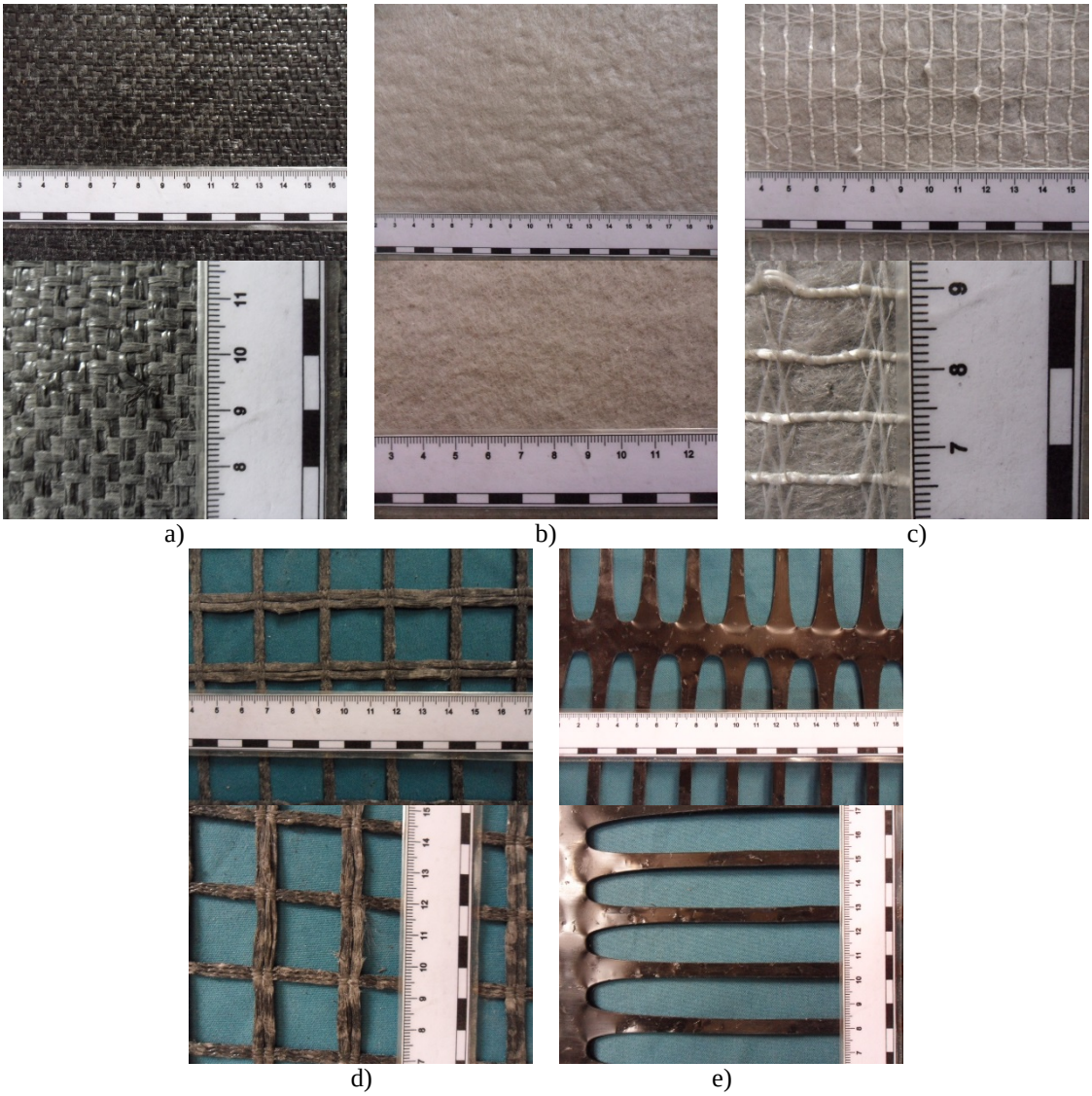

Figure 6. Examples of the visual inspection of specimens submitted to laboratory mechanical damage (LAB D): a) GTXw; b) GTXn; c) GCR; d) GGRw; e) GGRu.

Many of the geosynthetics exhibited puncturing, due to the contact of the aggregate particles with the surface of the geosynthetics during the mechanical damage test (Table 4). The least affected geosynthetic was GGRb, with no significant changes observed. For GTXw there was some localised evidence of fibre cutting and fibrillation of its PP tapes (Figure 6a). The surface of GTXn showed evidence of some puncturing (Figure 6b). After the mechanical damage induced in laboratory, some yarns of the GCR were cut and/or locally detached from the geotextile backing and there was some puncturing of the geotextile backing (Figure 6c).

For the sheet materials (GTXw, GTXn and GCR) and for GGRw an accumulation of fine particles (resulting from the fragmentation of the synthetic aggregate) was also observed (Figure 6a to 6d). The coating of GGRw was removed during the mechanical damage test and some of the fibres below it were cut (Figure 6d). The surface of GGRu (Figure 6e) had some evidence of puncturing and some cuts, due to contact with the particles of aggregate. In general, the visual observation indicated there were some changes on the surface of the geosynthetics. These may have contributed to changing the skin friction available during relative movement between the geosynthetics and the soil.

Table 4. Summary of the visual observation of specimens of the six geosynthetics studied after mechanical damage associated with installation.

Geosynthetic	Observations after mechanical damage
GTXw	Some tapes were cut; some localised fibrillation of the surface of the tapes; accumulation of fine particles from the fragmentation of the synthetic aggregate.
GTXn	Localised puncture due to the particles of the synthetic aggregate; incrustation of fine particles resulting from fragmentation of the synthetic aggregate.
GCR	Detachment and cuts of some of the PET yarns; evidence of perforations in the geotextile backing; incrustation of fines (resulting from fragmentation of the synthetic aggregate) within the geotextile backing.
GGRw	Removal of the coating; some fibre cutting; incrustation of fine particles.
GGRb	No visible changes.
GGRu	Some puncturing; cuts along the surface of the geogrid.

4.2 Inclined plane shear tests

The results of the inclined plane shear tests for undamaged samples (UND) and samples submitted to mechanical damage induced in laboratory (LAB D) are summarised in Table 5.

Table 5. Summary of the inclined plane shear tests results (mean values and coefficient of variation, CV) of: friction angle of the soil-geosynthetic interface (ϕ_{50}^{stat}), friction angle for initiation of the sliding of the upper box (ϕ_0), displacement of the upper box for which the sudden sliding of the upper box initiates (d_S) and soil-geosynthetic coefficient of interaction (*f*) for inclined shear plane movement, for undamaged samples and samples submitted to mechanical damage in laboratory.

Geosynthetic	Sample	Test method	ϕ_{50}^{stat} Mean (°)	ϕ_{50}^{stat} CV⁺ (%)	ϕ_0 Mean (°)	ϕ_0 CV⁺ (%)	d_s Mean (mm)	d_s CV⁺ (%)	f (-)
GTXw	UND	1	34.49	3.51	30.75	13.68	4.84	26.55	0.69
	LAB D		36.00	3.50	34.00	1.96	2.15	23.05	0.73
GTXn	UND		39.52	2.97	22.96	12.16	10.63	1.52	0.82
	LAB D		38.89	0.71	22.91	12.12	24.94	48.02	0.81
GCR	UND		39.28	0.60	28.77	19.42	8.72	13.13	0.82
	LAB D		39.67	3.44	33.08	3.34	22.79	64.85	0.83
GGRw	UND	2	*40.39	-	29.92	4.73	*9.29	-	0.85
	LAB D		40.40	1.02	29.11	8.03	8.11	7.03	0.85
GGRb	UND	1	39.30	1.89	27.51	33.58	7.73	38.95	0.82
	LAB D		+39.96	+0.97	33.91	7.21	+7.34	+6.78	0.84
GGRu	UND	1	40.37	0.20	30.26	33.43	14.86	41.65	0.85
	LAB D		+41.13	+0.02	33.99	10.83	+7.65	+25.45	0.87

Test method: 1 – specimen on a rigid base; 2 – specimen on a lower box with soil | * Result for 1 specimen only (for the other specimens the maximum inclination allowed by the equipment was reached) | + Results for 2 specimens only (for the other specimen the maximum inclination allowed by the equipment was reached)

Mean values for the angle of friction of the soil-geosynthetic interface (ϕ_{50}^{stat}), the friction angle for initiation of the sliding of the upper box (ϕ_0) and the displacement of the upper box for which phase 3, non-stabilised sliding of the upper box, initiates (d_S) are included, together with the corresponding coefficients of variation (CV, in %). The angle of friction of the soil-geosynthetic interface (ϕ_{50}^{stat}) is determined from the inclination angle, β_{50}, of the apparatus at which the upper box slides to a displacement of 50 mm (Equation 4) and the initial friction angle (ϕ_0) is determined from the inclination angle for initiation of the sliding of the upper box (β_0) using Equation 5. Herein W_s is the vertical force acting on the interface and $F_r(\beta)$ is

301 the force required to restrain the empty upper box for an inclination of β. These equations were
302 adapted from EN ISO 12957-2 [2] allowing for the static-dynamic interpretation of the test
303 results proposed by Gourc and Reyes Ramirez [4].

$$\tan \phi_{50}^{stat} = \frac{W_s \cdot \sin \beta_{50} + F_r(\beta_{50})}{W_s \cdot \cos\ \beta_{50}} \quad (4)$$

$$\tan \phi_0 = \frac{W_s \cdot \sin \beta_0 + F_r(\beta_0)}{W_s \cdot \cos\ \beta_0} \quad (5)$$

304 The inclination angle for initiation of the sliding of the upper box (β_0) and the displacement of
305 the upper box for which the sudden sliding of the upper box initiates (d_S) are illustrated Figure
306 7; d_s was estimated as the inclination of the upper box for 1 mm displacement. Figure 8
307 summarises the displacement versus inclination graphs for all geosynthetics studied.
308

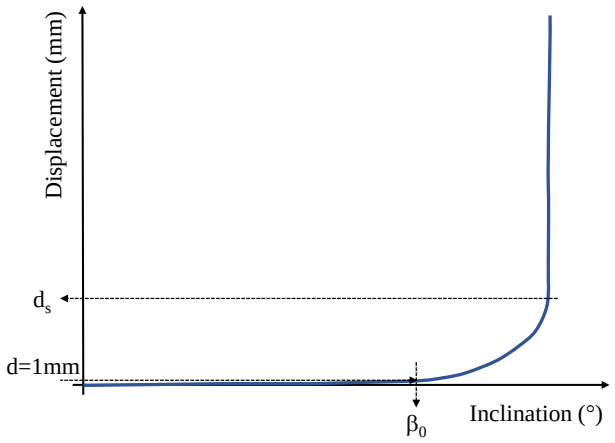

309
310 **Figure 7. Criteria used to estimate parameters β_0 and d_S from the inclined plane shear tests results.**
311

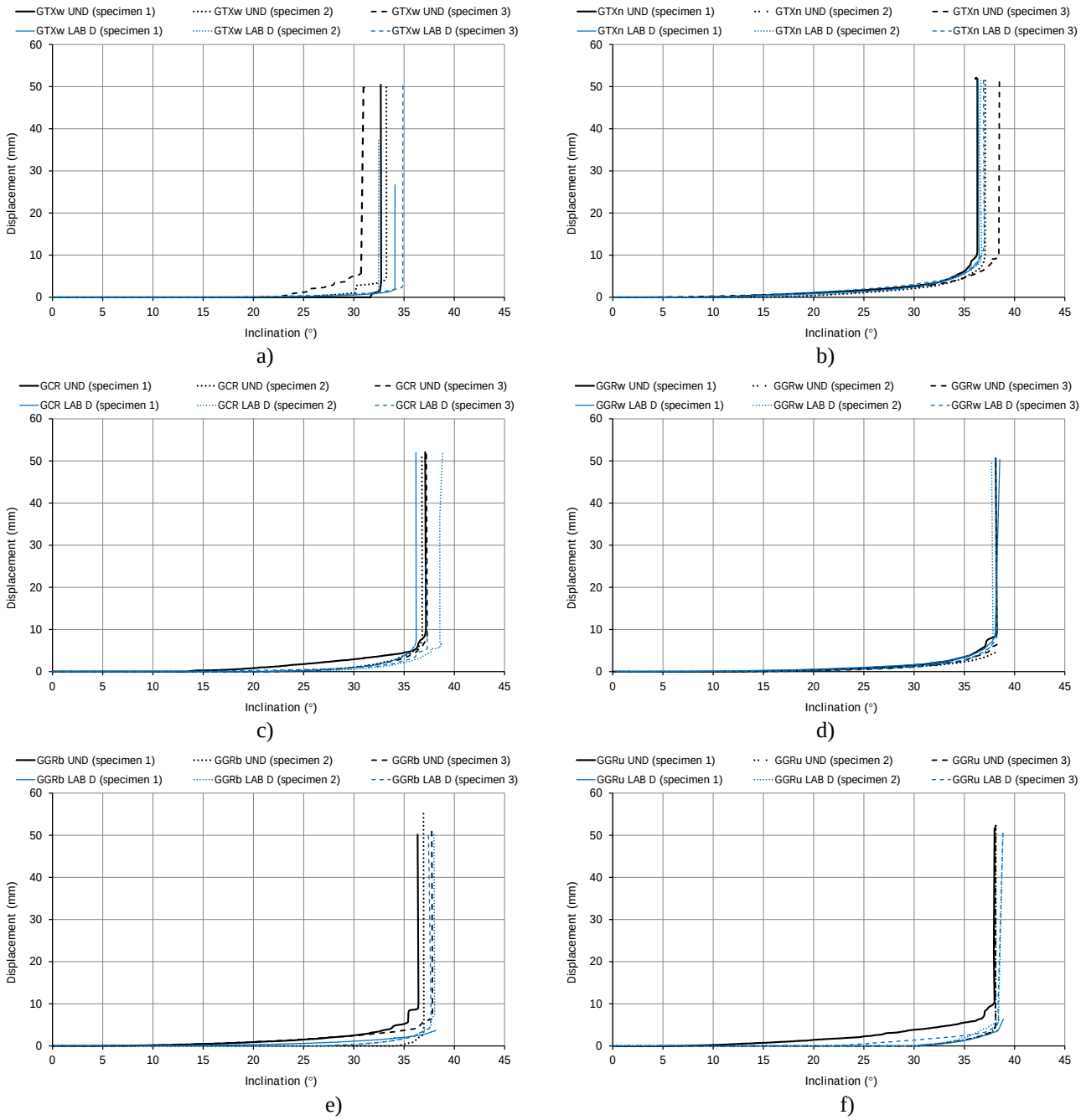

Figure 8. Inclined-shear plane response (displacement versus inclination curves) confined in soil (undamaged and after laboratory mechanical damage) for: a) GTXw; b) GTXn; c) GCR; d) GGRw; e) GGRb; f) GGRu.

4.2.1 Angle of friction of the soil-geosynthetic interface

For the undamaged samples, the angle of friction of the soil-geosynthetic interface (ϕ_{50}^{stat}) ranged between 34.5° (for GTXw) and 40.4° (for GGRw). The coefficient of variation (CV) values in Table 5 show that the repeatability of the tests was adequate, particularly for the angle

of friction of the soil-geosynthetic interface (ϕ_{50}^{stat}) obtained for the undamaged samples, with CV ranging between 3.5% and 0.2%. The value of ϕ_{50}^{stat} reported for GGRw is a low estimate of the true interface strength, as two of the specimens tested did not slide when the maximum inclination allowed by the equipment was reached.

Overall, after mechanical damage, the angle of friction of the soil-geosynthetic interface (Table 5) increased, as ϕ_{50}^{stat} ranged between 36.0°, for GTXw, to 41.1°, for GGRu. With the exception of GTXw (and possibly of GGRw, as there was only a low estimate of the interface strength for the undamaged sample), the angle of friction of the soil-geosynthetic interface (ϕ_{50}^{stat}) of the samples submitted to laboratory mechanical damage increased relatively to the corresponding value for the undamaged material (Table 5). The repeatability of results was also found adequate (represented by the corresponding coefficient of variation, CV, which ranged between 3.5% and 0.02%).

For the sheet-type materials studied (GTXw, GTXn and GCR), the strength mobilized on the soil-geosynthetic interface is skin friction. Thus, the results seem to indicate that the laboratory mechanical damage may have increased the roughness of the surface of these geosynthetics in contact with the soil. For the soil-geogrid interface, the soil-soil friction mobilised within the geogrid openings also contributes to the total strength mobilised. As in the inclined plane shear tests the geosynthetics are fixed, the relative movement occurring is the displacement of the upper box relatively to the geosynthetic (fixed on a rigid base or on a lower box with soil). As the laboratory damage tests did not influence the dimension of the geogrid apertures (confirmed during the visual observations of the damaged specimens), the differences in response observed for the damaged specimens are likely to be caused by different mobilisation of skin friction. Thus, for the geogrids it is also likely that the mechanical damage induced led to an increased roughness of their surface.

343 **4.2.2 Sliding mechanism**

344 To understand better the response of the soil-geosynthetic interfaces studied in inclined plane
345 shear movement, the sliding mechanisms were also analysed, assessing the influence of the
346 mechanical damage induced on those mechanisms.

347 All geosynthetics exhibited a gradual sliding. In some cases, there was a stick slip sliding
348 (not always clearly visible in Figure 8). Most undamaged samples of the geosynthetics studied
349 exhibited two types of gradual sliding during phase 2 – progressive and stick-slip. For example
350 for GGRb UND (Figure 8e), specimens 1 and 3 exhibited a stick –slip, while for specimen 2
351 the transitory phase was progressive. This seems to indicate that the inclined plane shear test
352 method does not lead to repeatable sliding mechanisms, even for undamaged specimens. The
353 only exception was GTXw UND, with the three specimens tested exhibiting stick-slip sliding
354 during phase 2.

355 After mechanical damage, all specimens of GTXw exhibited a progressive sliding during
356 phase 2. This seems to indicate that the changes and the accumulation of fines on the
357 geosynthetic surface are likely to have influenced the sliding mechanism developing during the
358 inclined plane shear test for this geosynthetic. Except for GTXn (2 specimens) and GGRb (2
359 specimens), all other specimens previously submitted to mechanical damage exhibited a
360 progressive sliding (phase 2). These responses seem to confirm the trend observed for GTXw,
361 with a progressive sliding for phase 2 more prevalent for damaged specimens.

362 The initial friction angle, ϕ_0 (Table 5), which represents the initiation of the sliding of
363 the upper box, increased after mechanical damage, except for GTXn (with no significant
364 change) and GGRw (slight decrease). However, for the undamaged samples, this quantity
365 exhibited higher scatter (CV ranging between 4.7% and 33.6%) than after damage (CV ranging
366 between 2.0% and 12.1%). These results seem to indicate that the mechanical damage reduces
367 the heterogeneity of responses observed.

The displacement of the upper box for which phase 3 (non-stabilised sliding of the upper box) initiates (d_S) also had a large scatter for the undamaged samples, increasing significantly after damage, in particular for GTXn and GCR. Analysing only results for three valid specimens, the laboratory mechanical damage was likely to have contributed to increasing the scatter for the upper box displacement that initiates its sudden sliding (d_s), with CV values between 1.5% and 41.7% for the undamaged samples and between 7.0% and 64.9% after mechanical damage.

4.2.3 Influence of the geosynthetic structure

To analyse the influence of the geosynthetic structure, the results for GTXn, GCR and GGRw were compared, as these geosynthetics have similar nominal tensile strength (ranging between 55 and 58 kN/m) and different structures.

The interface strength properties obtained for these three geosynthetics were quite similar, with the angle of friction for the soil-geosynthetic interface (undamaged sample) ranging between 39.3° (GCR) and 40.4° (GGRw). The higher interface strength mobilised for GGRw is likely to be related to the soil-soil strength mobilised within the openings of the geogrid, while for GTXn and GCR (sheet materials) only skin friction is mobilised. After mechanical damage the interface strength did not change significantly, ranging between 38.9° (GTXn) and 40.4° (GGRw). For GGRw, a significant part of the strength measured was mobilised within the openings (soil-soil friction) and, thus, there were no real changes in interface strength after damage (regardless of the changed surface of the geogrid, Figure 6d). For GTXn the interface strength was reduced after mechanical damage, showing that the skin friction mobilised decreased. This is likely to be caused by the accumulation of fines on the surface of GTXn (Figure 6b). For GCR the mean value of the interface strength increased after damage, although the scatter of responses also increased.

Although the three geosynthetics have the same nominal tensile strength, their tensile strength is often higher than the value stated on their technical datasheets. Rosete et al. [23] presented tensile strength values for these geosynthetics both undamaged and after laboratory mechanical damage. The tensile strength of the undamaged samples was 70.3 kN/m for GTXn, 54.6 kN/m for GCR and 44.4 kN/m for GGRw. Thus, although apparently the three geosynthetics have the same nominal strength, GTXn was found much stronger than stated by its producer. Because of this, the tensile strength after laboratory mechanical damage was higher than the nominal tensile strength stated in the product datasheet: after laboratory mechanical damage the tensile strength values reduced to 64.7 kN/m for GTXn, 30.2 kN/m for GCR and 36.4 kN/m for GGRw. This is likely to have influence the inclined plane shear response of GTXn.

The mechanical damage induced is likely to affect the tensile response of the geosynthetics more than their interface strength. For example, the mechanical damage partially removed the protective polymeric coating of GGRw and induced some fibre cutting. Such changes affected the tensile elements of this geosynthetic, thus influencing its tensile response. Additionally, the surface of the geogrid was changed, which may have contributed to altering the skin friction available at its surface (this is further discussed in section 4.2.4). For GCR, cutting of the yarns influenced its tensile strength; this is likely to have less impact on the soil-geosynthetic interface strength. Thus, the structure of the geosynthetics had a higher impact on their tensile response after mechanical damage than on the soil-geosynthetic interface in inclined plane shear.

4.2.4 Influence of the type of geogrid

Herein three different geogrids were studied. For some of the tests, particularly with GGRw UND and GGRb and GGRu LAB D, the limit of the equipment was reached and the corresponding values of the soil-geogrid interface angle of friction reported in Table 5 are

lower estimates of the true interface strength. For the values obtained, and for the undamaged samples, GGRb had the lowest interface strength (ϕ_{50}^{stat}=39.3°), while GGRw and GGRu had similar higher values (ϕ_{50}^{stat}=40.4°). These differences were likely caused by the different surface roughness of the geogrids and by the different solid and aperture areas available to mobilise skin friction and soil-soil friction, respectively.

As discussed in section 4.2.1, the mechanical damage induced on the geogrids may have led to an increased roughness of their surface. The test results were used to quantify the expected increase in surface roughness. Assuming a uniform normal stress distribution at the soil-geogrid interface (and ignoring any dynamic effects of the sliding process), Equation 6 was used to estimate the two components of strength mobilised in the soil-geosynthetic interface during shear (herein represented as ϕ_{50}^{stat}): the soil-soil friction mobilised within the openings of the geogrid ($\alpha_o \cdot \tan \phi_{ss}$); and the skin friction mobilised along the solid surface of the geogrid in contact with the soil ($\alpha_s \cdot \tan \phi_{sg}$). The solid fraction of the geogrid in the contact with the soil in the upper box is represented by α_s, while α_o represents the open fraction of the geogrid (i.e., the area of its apertures); ϕ_{ss} is the angle of friction of the soil and ϕ_{sg} represents the friction angle mobilised in the solid area of the geogrid. These values are summarised in Table 6.

$$\tan \phi_{50}^{stat} = \alpha_o \cdot \tan \phi_{ss} + \alpha_s \cdot \tan \phi_{sg} \quad (6)$$

Table 6. Components of strength mobilised in the soil-geogrid interface in inclined plane shear (ϕ_{50}^{stat}) for GGRw, GGRb and GGRu: open fraction of the geogrid, i.e., the apertures (α_o); solid fraction of the geogrid in the contact with the soil in the upper box (α_s); angle of friction of the soil (ϕ_{ss}); angle of friction mobilised in the solid area of the geogrid (ϕ_{sg}).

Geosynthetic	Sample	α_o	α_s	ϕ_{50}^{stat}	ϕ_{ss}	ϕ_{sg}
		(-)	(-)	(°)	(°)	(°)
GGRw	UND	0.65	0.35	*40.39	42.5	36.09
	LAB D			40.40		36.12
GGRb	UND	0.87	0.13	39.30		9.30
	LAB D			+39.96		17.39
GGRu	UND	0.68	0.32	40.36		35.32
	LAB D			+41.13		38.02

* Result for 1 specimen only (for the other specimens the maximum inclination allowed by the equipment was reached) | + Results for 2 specimens only (for the other specimen the maximum inclination allowed by the equipment was reached)

The open fraction of GGRw and GGRu is comparable and smaller than for GGRb. Thus, for GGRb a large proportion of the interface strength measured in the inclined plane shear test (ϕ_{50}^{stat}), was due to soil-soil friction within the geogrid apertures (open fraction α_o=0.87). For GGRw and GGRu a similar proportion of the interface strength measured in the inclined plane shear test (ϕ_{50}^{stat}), was due to skin friction mobilised along their surface (solid fraction α_s=0.65 for GGRw and α_s=0.68 for GGRu). The results for the samples of GGRb and GGRu submitted to mechanical damage are low estimates of ϕ_{50}^{stat}, as some of the specimens did not slide when the maximum inclination of the box was reached. For the three geogrids, the friction mobilised in the solid area of the geogrid increased after mechanical damage. The results contradict the visual observations of the damaged samples, as GGRb, which exhibited no significant change (Table 4), had the largest increase in the skin friction mobilised along the solid surface of the geogrid in contact with the soil. This may indicate that the surface of GGRb and GGRu was more affected by mechanical damage than apparent from the (naked eye) visual inspection.

457 Nevertheless, the estimate of ϕ_{sg} for GGRb confirms that its surface is much smoother than
458 GGRw and GGRu.

459 **4.2.5 Coefficient of interaction in inclined plane shear**

460 The values for the soil-geosynthetic coefficient of interaction in inclined plane shear (*f*,
461 Equation 7) are included in Table 5.

$$f = \tan \phi_{50}^{stat} \quad (7)$$

462 For the undamaged geosynthetics, the coefficient of interaction in inclined plane shear ranged
463 between 0.67 (GTXw) and 0.85 (GGRw and GGRu), while after mechanical damage it ranged
464 between 0.73 (GTXw) and 0.87 (GGRu). For GTXw, GCR, GGRb and GGRu the soil-
465 geosynthetic interface strength was higher after mechanical damage induced in laboratory,
466 represented by the increase in the corresponding coefficient of interaction, *f*. For GTXn the
467 opposite trend was observed (although for a small reduction of the coefficient of interaction),
468 while for GGRw there was no change in *f*.

469 The results seem to indicate that in most cases the mechanical damage caused an
470 increase in the skin friction available, as discussed previously. This is likely to have been
471 caused by the puncturing (GCR and GGRu) and the accumulation of some fines within the
472 surface of some of the geosynthetic (GTXw and GCR), fibre cutting (GGRw) and/or fibrillation
473 of the tapes (GTXw).

474 **4.3 Reduction factor for laboratory mechanical damage**

475 The results of the inclined shear plane test were used to estimate reduction factors for
476 mechanical damage associated with installation for the soil-geosynthetic interface strength in
477 inclined plane shear movement. Such reduction factors, $RF_{LabD,ips}$ (Equation 8) were

478 determined as the ratio between the coefficient of friction soil - undamaged geosynthetic
479 (tan ϕ_{50}^{stat} $_{UND}$) and that of soil – damaged geosynthetic (tan ϕ_{50}^{stat} $_{DAM}$).

$$RF_{labD,ips} = \frac{\tan \phi_{50\ UND}^{stat}}{\tan \phi_{50\ DAM}^{stat}} \quad (8)$$

480 A reduction factor to allow for mechanical damage associated with installation for the tensile
481 strength ($RF_{LabD,tensile}$) of the geosynthetics was also calculated (Equation 9) as the ratio
482 between the tensile strength of an undamaged sample ($T_{max\ UND}$) of a geosynthetic to that
483 measured after mechanical damage ($T_{max\ DAM}$).

$$RF_{LabD,tensile} = \frac{T_{\max UND}}{T_{\max DAM}} \quad (9)$$

484 These tensile tests results were obtained using wide-width tensile tests (EN ISO 10319 [24])
485 where the strains were measured using video-extensometers and refer to five valid specimens.
486 The data for GTXn, GCR, GGRw, GGR were presented by Rosete et al. [23]. For some of
487 geosynthetics, two sets of results are available, depending on the maximum pressure applied
488 during the mechanical damage tests – 500 kPa (EN ISO 10722 [21]) or 900 kPa (ENV ISO
489 10722-1 [25]).

490 The reduction factors for mechanical damage associated with installation are
491 summarised in Table 7. The minimum value to be used for the reduction factors is 1.0. The
492 reduction factors for mechanical damage for the inclined plane shear tests ranged between 0.88
493 (GTXw) and 1.07 (GGRu). For the two geotextiles studied (GTXw and GTXn) $RF_{LabD,ips}$ is
494 lower than the minimum value of 1.0, reflecting an increase in interface strength after
495 mechanical damage. The causes for such increase have been discussed in previous sections.
496 The results obtained for the six geosynthetics studied indicate that the angle of friction of the
497 soil-geosynthetic interface (ϕ_{50}^{stat}) was not significantly affected by the mechanical damage
498 induced in laboratory.
499

Table 7. Reduction factors for mechanical damage associated with installation obtained from inclined plane shear tests ($RF_{LabD,ips}$) and from tensile tests ($RF_{LabD,tensile}$).

Geosynthetic	$RF_{LabD,ips}$	$RF_{LabD,tensile}$	
	500 kPa	500 kPa	900 kPa
GTXw	1.14		2.32
GTXn	1.02	1.09	1.20
GCR	0.99	1.64	1.99
GGRw	0.96	1.22	1.27
GGRb	0.98		0.99
GGRu	0.94		1.09

For comparable conditions in the mechanical damage tests (maximum pressure of 500 kPa), for most geosynthetics the reduction factor for mechanical damage for the inclined plane shear movement ($RF_{LabD,ips}$) is lower than for the tensile force ($RF_{LabD,tensile}$). However, for GGRb, while the tensile strength increased after mechanical damage (for maximum applied pressure of 900 kPa), the angle of friction of the soil-geosynthetic interface decreased after mechanical damage. Thus, while for GGRb the reduction factor for mechanical damage for the tensile strength is too optimistic, for the other geosynthetics studied the reduction factor for the tensile strength is too conservative relatively to $RF_{LabD,ips}$.

Pinho-Lopes et al. [20] have studied the soil-geosynthetic interface in inclined plane shear movement of GTXw after field installation damage under real conditions. The corresponding reduction factor for installation damage ranged between 1.11 and 1.12, depending on the compaction energy used. Thus, for GTXw and for the test conditions reported herein, the mechanical damage induced in laboratory could not replicate the damage induced in field under real conditions and is conservative. Pinho-Lopes et al. [20] also studied a geosynthetic similar to GGRw. For that material (which had different opening sizes and nominal properties but a similar structure and manufacturing process), the reduction factor for installation damage in inclined plane shear after field installation damage ranged between 0.99 and 1.01, depending on the compaction energy used. In this case, the mechanical damage

induced in laboratory was able to replicate the changes in inclined plane shear strength (ϕ_{50}^{stat}) measured after field installation under real conditions.

5 CONCLUSIONS

In this paper the inclined plane shear response of six geosynthetics in contact with a granular soil was analysed, particularly the influence of mechanical damage associated with installation on the soil-geosynthetic interaction in this type of relative movement. From the results the main conclusions are:

- For the undamaged samples, the angle of friction of the soil-geosynthetic interface ranged between 34.5° and 40.4°; after mechanical damage that angle increased (ranging between 36.0° and 41.1°). In both types of samples, the angle of friction of the soil-geosynthetic interface exhibited adequate repeatability.
- For the materials and test conditions considered, the inclined plane shear test method did not lead to repeatable sliding mechanisms, particularly during the transitory phase. For the undamaged geosynthetics, both progressive and stick-slip sliding were observed for specimens of a same sample. After mechanical damage, many specimens exhibited a progressive sliding (phase 2). After mechanical damage, the initiation of the sliding of the upper box exhibited a reduced scatter, while the displacement for the initiation of the non-stabilised sliding of the upper box, phase 3) was more varied.
- The structure of the geosynthetic influenced the inclined plane shear response observed; the planar geosynthetics exhibited lower interface strength than the geogrid with a similar nominal strength. The structure also influenced the effects of the mechanical damage of the geosynthetics. Hence, the structure of the geosynthetic also affected the inclined plane shear response after mechanical damage.

- The friction mobilised in the solid area of the geogrids increased after mechanical damage, indicating an increased roughness of those surfaces due to mechanical damage. Such increases depended on the type of geogrid and on the consequences of mechanical damage.
- Overall, the results showed that the mechanical damage caused an increase in the skin friction available, due to the observed damage mechanisms (puncturing, accumulation of some fines within the surface of the geosynthetics, fibre cutting and/or fibrillation of tapes). The laboratory mechanical damage affected the soil-geosynthetic interface strength and the sliding mechanisms observed.
- The reduction factors for mechanical damage associated to installation showed that the interface strength did not change significantly. The reduction factor obtained from tensile tests was, in most cases, too conservative to represent the influence of the mechanical damage on the soil-geosynthetic interface strength in inclined plane shear movement. The structure of the geosynthetics had a higher impact on their tensile response after mechanical damage than on the soil-geosynthetic interface in inclined plane shear.
- For the interface strength in inclined shear plane movement, the mechanical damage induced in laboratory of the woven geotextile was conservative compared to field installation damage, while for the woven geogrid the mechanical damage induced in laboratory was within the range of damage induced in the field.

Thus, despite some heterogeneity of responses observed, particularly for the sliding mechanisms, the standardised laboratory tests to induce mechanical damage in laboratory seem to be able to represent the effect of the mechanical damage associated with installation on the inclined plane shear response of soil-geosynthetic interfaces.

NOTATION

Basic SI units are given in parentheses.

c'	Drained cohesion (Pa)
d	Displacement (m)
d_{2kPa}	Nominal thickness (m)
d_{long}	Thickness of longitudinal ribs (m)
d_{trans}	Thickness of transverse ribs (m)
D_{10}	Largest particle size in the smallest 10% of the soil particles (m)
D_{50}	Largest particle size in the smallest 50% of the soil particles (m)
D_{max}	Maximum soil particle size (m)
d_s	Displacement of the upper box in the inclined-plane shear test for which the sudden movement of the box occurs (m)
f	Soil-geosynthetic coefficient of interaction (-)
$F_r(\beta)$	Force required to restrain the empty upper box for an inclination of β (N)
g	acceleration of gravity (m^2/s)
I_D	Soil relative density (%)
m_b	mass of the upper box (kg)
m_s	is the mass of soil in the upper box (kg)

$RF_{LABD,ips}$	Reduction factor for mechanical damage obtained from the inclined plane shear tests (-)
$RF_{LABD,tensile}$	Reduction factor for mechanical damage obtained from the tensile tests (-)
T_{guide}	Tangential component of the reaction of the guidance system (N)
$T_{max\ DAM}$	Mean value of the tensile strength of the damaged sample (N/m)
$T_{max\ UND}$	Mean value of the tensile strength of the undamaged sample (N/m)
W_s	Vertical force acting on the interface (N)
α_o	open fraction of the geogrid (dimensionless)
α_s	solid fraction of the geogrid in the contact with the soil in the upper box (dimensionless)
β	Inclination of the upper box in the inclined-plane shear tests, relatively to the horizontal (°)
β_0	Inclination angle of the upper box in the inclined-plane shear tests, relatively to the horizontal, at the static limit equilibrium (°)
β_{50}	Inclination angle of the upper box in the inclined-plane shear tests, relatively to the horizontal, to a displacement of 50mm (°)
β_s	Inclination angle of the upper box in the inclined-plane shear tests, relatively to the horizontal, for non-stabilized sliding (°)
ϕ'	Drained friction angle (º)

ϕ_0	Static or initial angle of friction of the soil-geosynthetic interface (°)
ϕ_{50}^{stat}	Angle of friction of the soil-geosynthetic interface from EN ISO 1257-2 (BSI, 2005) (°)
$\phi_{50}^{stat}{}_{\text{DAM}}$	Mean value of the angle of friction for the soil-geosynthetic interface for damaged samples (°)
$\phi_{50}^{stat}{}_{\text{UND}}$	Mean value of the angle of friction for the soil-geosynthetic interface for undamaged samples (°)
ϕ_{lim}	Limit angle of friction of the soil-geosynthetic interface for uniformly accelerated movement (°)
ϕ_{sg}	Angle of friction mobilised in the solid area of the geogrid (°)
ϕ_{ss}	Angle of friction of the soil (°)
μ	Mass per unit area (kg/m^2)
γ	Soil unit weight (N/m^3)
γ_c	Constant acceleration of the upper box (m^2/s)
CV	Coefficient of variation
GCR	Geocomposite
GGR	Geogrid
GTX	Geotextile
HDPE	High density polyethylene

LAB D Damaged in laboratory

UND Undamaged

PET Polyester

PP Polypropylene

ACKNOWLEDGEMENTS

This work was supported by projects: POCI-01-0145-FEDER-007457-CONSTRUCT (R&D Institute for Structures and Construction) funded by FEDER through COMPETE2020 - Programa Operacional Competitividade e Internacionalização (POCI) and by national funds through FCT - Fundação para a Ciência e a Tecnologia. The authors would like to thank the financial support of FCT (Fundação para a Ciência e para a Tecnologia) - Portugal, Research Project PTDC/ECM/099087/2008 and COMPETE, Research Project FCOMP-01-0124-FEDER-009724. The authors acknowledge Pedro Mendonça Lopes for performing most tests reported herein.

REFERENCES

[1] E.M. Palmeira, N.R. Lima Jr, L.G.R. Mello, Interaction Between Soils and Geosynthetic Layers in Large-Scale Ramp Tests, Geosynthetics Int. 9(2) (2002) 149-187. DOI 10.1680/gein.9.0214

[2] BSI EN ISO 12957-2:2005. Geosynthetics - Determination of friction characteristics -- Part 2: Inclined plane test. BSI (2005), London, UK.

[3] R. Reyes Ramirez, J.P. Gourc, Use of the inclined plane test in measuring geosynthetic interface friction relationship, Geosynthetics Int. 10(5) (2003) DOI 165–175. 10.1680/gein.2003.10.5.165

588 [4] J.P. Gourc, R. Reyes Ramirez, Dynamics-based interpretation of the interface friction test
589 at the inclined plane, Geosynthetics Int. 11(6) (2004) 439-454. DOI
590 10.1680/gein.2004.11.6.439
591 [5] L. Briançon, Stabilité sur pentes des dispositifs geosynthetiques: caractérisation du
592 frottement aux interfaces et applications, PhD thesis, University of Bordeaux, France (2001)
593 (*in French*).
594 [6] H.N. Pitanga, J.P. Gourc, O.M. Vilar, Interface shear strength of geosynthetics: evaluation
595 and analysis of inclined plane test, Geotext. Geomembr. 27(6) (2009) 435-446. DOI
596 10.1016/j.geotexmem.2009.05.003
597 [7] L. Briançon, H. Girard, J.P. Gourc, A new procedure for measuring geosynthetic friction
598 with an inclined plane, Geotext. Geomembr. 29 (5) (2011) 472-482. DOI
599 10.1016/j.geotexmem.2011.04.002
600 [8] T.M. Allen, R.J. Bathurst, Characterization of geosynthetic load-strain behavior after
601 installation damage, Geosynthetics Int. 1(2) (1994) 181-199. DOI 10.1680/gein.1.0008
602 [9] R. Hufenus, R. Ruegger, D. Flum, I.J. Sterba, Strength reduction factors due to installation
603 damage of reinforcing geosynthetics, Geotext. Geomembr. 23(5) (2005) 401-424. DOI
604 10.1016/j.geotexmem.2005.02.003
605 [10] C.-C. Huang, S.-L. Chiou, Investigation of installation damage of some geogrids using
606 laboratory tests, Geosynthetics Int. 13(1) (2006) 23–35. DOI 10.1680/gein.2006.13.1.23
607 [11] C.-C. Huang, Z.-H. Wang, Installation damage of geogrids: influence of load intensity,
608 Geosynthetics Int. 14(2) (2007) 65–75. DOI 10.1680/gein.2007.14.2.65
609 [12] M. Pinho-Lopes, M.L. Lopes, Tensile properties of geosynthetics after installation
610 damage, Environ. Geotech. (ICE), 1(3) (2014) 161-178. DOI 10.1680/envgeo.13.00032

611 [13] T.M. Allen, R.J. Bathurst, Combined allowable strength reduction factor for geosynthetic
612 creep and installation damage. Geosynthetics Int. 3(3) (1996) 407-439. DOI
613 10.1680/gein.3.0069
614 [14] J.H. Greenwood, The effect of installation damage on the long-term design strength of a
615 reinforcing geosynthetic, Geosynthetics Int. 9(3) (2002) 247-258. DOI 10.1680/gein.9.0217
616 [15] S.D. Cho, K.W. Lee, D.A. Cazzuffi, H.Y. Jeon, Evaluation of combination effects of
617 installation damage and creep behavior on long-term design strength of geogrids. Polym.
618 Test. 25(6) (2006) 819-828. DOI 10.1016/j.polymertesting.2006.04.007
619 [16] H.-Y. Jeon, A. Bouazza, Experimental investigation of installation damage for geogrids,
620 Proceedings of the Institution of Civil Engineers - Ground Improvement 163 (4) (2010) 197-
621 205. DOI 10.1680/grim.2010.163.4.197
622 [17] R.J. Bathurst, Y. Miyata, Reliability-based analysis of combined installation damage and
623 creep for the tensile rupture limit state of geogrid reinforcement in Japan, Soils Found. 55(2)
624 (2015) 437–446. DOI 10.1016/j.sandf.2015.02.017
625 [18] M. Pinho-Lopes, A.M. Paula, M.L. Lopes, Long-term response and design of two
626 geosynthetics: effect of field installation damage, Geosynthetics Int. 25(1) (2018) 98-117.
627 DOI 10.1680/jgein.17.00036
628 [19] M. Pinho-Lopes, A.M. Paula, M.L. Lopes, Pullout response of geogrids after installation,
629 Geosynthetics Int. 22(5) (2015) 339-354. DOI 10.1680/gein.15.00016
630 [20] M. Pinho-Lopes, A.M. Paula, M.L. Lopes, Soil–geosynthetic interaction in pullout and
631 inclined-plane shear for two geosynthetics exhumed after installation damage,
632 Geosynthetics Int. 23(5) (2016) 331-347. DOI doi:10.1680/jgein.16.00001
633 [21] BSI EN ISO 10722:2007 – Geosynthetics. Index test procedure for the evaluation of
634 mechanical damage under repeated loading. Damage caused by granular material BSI
635 (2007), London, UK.

636 [22] P.C. Lopes, M.L. Lopes, M.P. Lopes, Shear behaviour of geosynthetics in the inclined
637 plane test – influence of soil particle size and geosynthetic structure, Geosynthetics Int. 8
638 (4) (2001) 327-342. DOI 10.1680/gein.8.0198
639 [23] A. Rosete, P. Mendonça Lopes, M. Pinho-Lopes, M.L Lopes, Tensile and hydraulic
640 properties of geosynthetics after mechanical damage and abrasion laboratory tests,
641 Geosynthetics Int. 20(5) (2013) 358-374. DOI 10.1680/gien.13.00022
642 [24] BSI EN ISO 10319:2008: Geosynthetics. Wide-width tensile test. BSI (2008), London,
643 UK.
644 [25] BSI ENV ISO 10722-1 (1998). Geotextiles and geotextile-related products - Procedure
645 for simulating damage during installation – Part 1: Installation in granular materials. BSI
646 (1998), London, UK.
647 .

TABLES

Table 1 – Characteristics of the geosynthetics tested.

Property	Geosynthetic					
	GTXw	GTXn	GCR	GGRw	GGRb	GGRu
Polymer	PP	PP	PET/PP	PET	PP	HDPE
Mass per unit area, μ (g/m^2)	320	1000	321	380	530	450
Nominal thickness, d_{2kPa} (mm)	1.2	7.2	2.1	1.7	-	-
Thickness of longitudinal ribs, d_{long} (mm)	-	-	-	1.6	2.2	1.1
Thickness of transverse ribs, d_{trans} (mm)	-	-	-	1.6	1.4	2.7
Mean grid openings dimensions (mm x mm)	-	-	-	25×25	33×33	22×235
Short-term tensile strength (kN/m)	65	55	58	58	40	68
Strain at maximum load (%)	11.0	105.0	10.0	10.5	11.0	9.0

Table 2 - Test program implemented and number of specimens tested.

Geosynthetic	Sample	Mechanical damage (Adapted from EN ISO 10722)	Inclined plane shear (EN ISO 12957-2)
GTXw	UND	–	3
	LAB D	3	3
GTXn	UND	–	3
	LAB D	3	3
GCR	UND	–	3
	LAB D	3	3
GGRw	UND	–	3
	LAB D	3	3
GGRb	UND	–	3
	LAB D	3	3
GGRu	UND	–	3
	LAB D	3	3

GTXw – woven geotextile | GTXn – nonwoven geotextile | GCR – reinforcement geocomposite

GGRw – woven geogrid | GGRb – biaxial extruded geogrid | GGRu – uniaxial extruded geogrid

UND – undamaged | LAB D – submitted to mechanical damage in laboratory

Table 3 – Properties of the soil used in the inclined plane shear tests.

% Fines (<0.074mm) (%)	D_{10} (mm)	D_{50} (mm)	D_{max} (mm)	$\gamma^{\#}$ (kN/m^3)	$\phi'^{\#}$ (^{o})	$c'^{\#}$ (^{o})
3.63	0.19	2.67	10.00	17.61	42.5	8.49

$^{\#}$ for a relative density I_D=50%

Table 4. Summary of the visual observation of specimens of the six geosynthetics studied after mechanical damage associated with installation.

Geosynthetic	Observations after mechanical damage
GTXw	Some tapes were cut; some localised fibrillation of the surface of the tapes; accumulation of fine particles from the fragmentation of the synthetic aggregate.
GTXn	Localised puncture due to the particles of the synthetic aggregate; incrustation of fine particles resulting from fragmentation of the synthetic aggregate.
GCR	Detachment and cuts of some of the PET yarns; evidence of perforations in the geotextile backing; incrustation of fines (resulting from fragmentation of the synthetic aggregate) within the geotextile backing.
GGRw	Removal of the coating; some fibre cutting; incrustation of fine particles.
GGRb	No visible changes.
GGRu	Some puncturing; cuts along the surface of the geogrid.

Table 5. Summary of the inclined plane shear tests results (mean values and coefficient of variation, CV) of: friction angle of the soil-geosynthetic interface (ϕ_{50}^{stat}), friction angle for initiation of the sliding of the upper box (ϕ_0), displacement of the upper box for which the sudden sliding of the upper box initiates (d_s) and soil-geosynthetic coefficient of interaction (f) for inclined shear plane movement, for undamaged samples and samples submitted to mechanical damage in laboratory.

Geosynthetic	Sample	Test method	ϕ_{50}^{stat}		ϕ_0		d_s		f
			Mean (°)	CV+ (%)	Mean (°)	CV+ (%)	Mean (mm)	CV+ (%)	(-)
GTXw	UND	1	34.49	3.51	30.75	13.68	4.84	26.55	0.69
	LAB D		36.00	3.50	34.00	1.96	2.15	23.05	0.73
GTXn	UND		39.52	2.97	22.96	12.16	10.63	1.52	0.82
	LAB D		38.89	0.71	22.91	12.12	24.94	48.02	0.81
GCR	UND		39.28	0.60	28.77	19.42	8.72	13.13	0.82
	LAB D		39.67	3.44	33.08	3.34	22.79	64.85	0.83
GGRw	UND	2	*40.39	-	29.92	4.73	*9.29	-	0.85
	LAB D		40.40	1.02	29.11	8.03	8.11	7.03	0.85
GGRb	UND	1	39.30	1.89	27.51	33.58	7.73	38.95	0.82
	LAB D		+39.96	+0.97	33.91	7.21	+7.34	+6.78	0.84
GGRu	UND	1	40.37	0.20	30.26	33.43	14.86	41.65	0.85
	LAB D		+41.13	+0.02	33.99	10.83	+7.65	+25.45	0.87

Test method: 1 – specimen on a rigid base; 2 – specimen on a lower box with soil | * Result for 1 specimen only (for the other specimens the maximum inclination allowed by the equipment was reached) | + Results for 2 specimens only (for the other specimen the maximum inclination allowed by the equipment was reached)

Table 6. Components of strength mobilised in the soil-geogrid interface in inclined plane shear (ϕ_{50}^{stat}) for GGRw, GGRb and GGRu: open fraction of the geogrid, i.e., the apertures (α_o); solid fraction of the geogrid in the contact with the soil in the upper box (α_s); angle of friction of the soil (ϕ_{ss}); angle of friction mobilised in the solid area of the geogrid (ϕ_{sg}).

Geosynthetic	Sample	α_o	α_s	ϕ_{50}^{stat}	ϕ_{ss}	ϕ_{sg}
		(-)	(-)	(°)	(°)	(°)
GGRw	UND	0.65	0.35	*40.39	42.5	36.09
	LAB D			40.40		36.12
GGRb	UND	0.87	0.13	39.30		9.30
	LAB D			+39.96		17.39
GGRu	UND	0.68	0.32	40.36		35.32
	LAB D			+41.13		38.02

* Result for 1 specimen only (for the other specimens the maximum inclination allowed by the equipment was reached) | + Results for 2 specimens only (for the other specimen the maximum inclination allowed by the equipment was reached)

Table 7. Reduction factors for mechanical damage associated with installation obtained from inclined plane shear tests ($RF_{LabD,ips}$) and from tensile tests ($RF_{LabD,tensile}$).

Geosynthetic	$RF_{LabD,ips}$	$RF_{LabD,tensile}$	
	500 kPa	500 kPa	900 kPa
GTXw	1.14		2.32
GTXn	1.02	1.09	1.20
GCR	0.99	1.64	1.99
GGRw	0.96	1.22	1.27
GGRb	0.98		0.99
GGRu	0.94		1.09

FIGURES

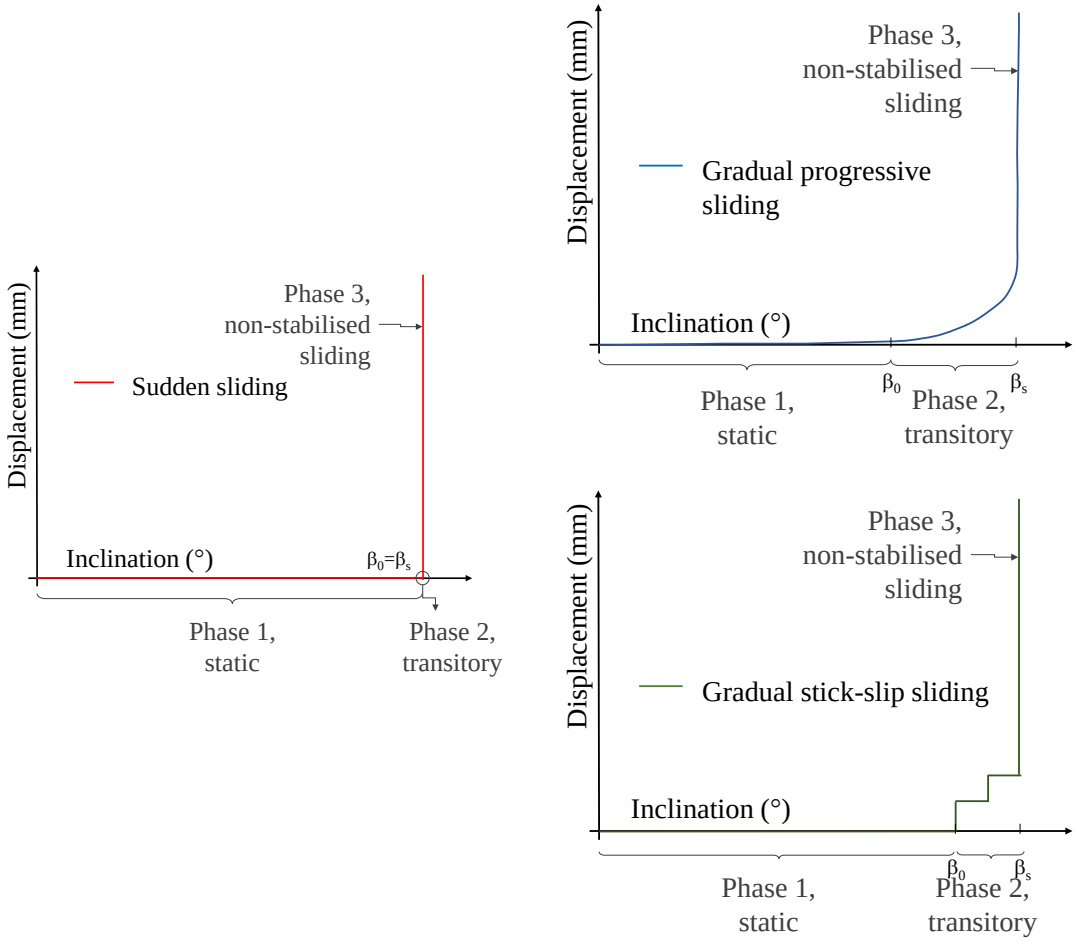

a) **b)**

Figure 1 – Schematic representation of the different sliding mechanisms typically observed in inclined plane shear tests with indication of the different sliding stages: a) sudden and b) gradual sliding (progressive and stick-slip) of the upper box.

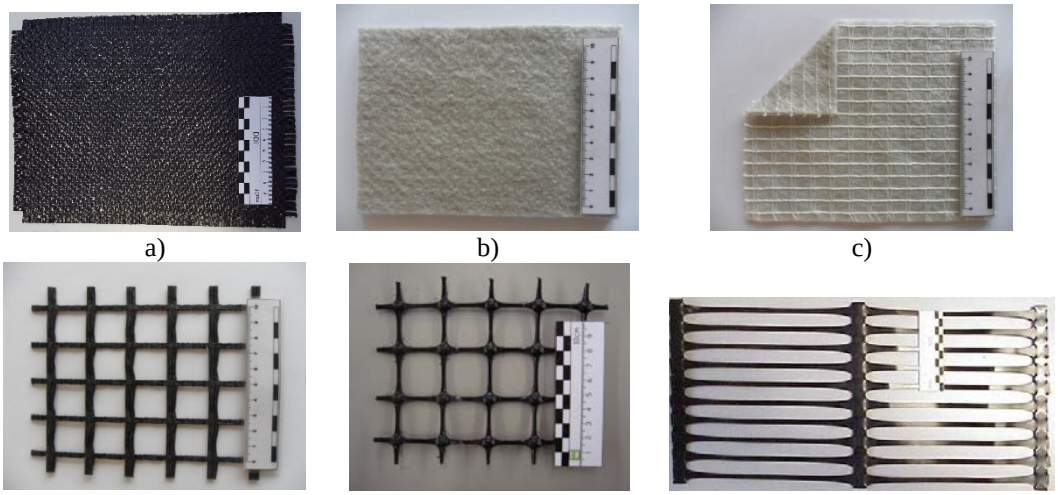

a) b) c)

d) e) f)

Figure 2 – Geosynthetics studied: a) GTXw; b) GTXn; c) GCR; d) GGRw; e) GGRb; f) GGRu.

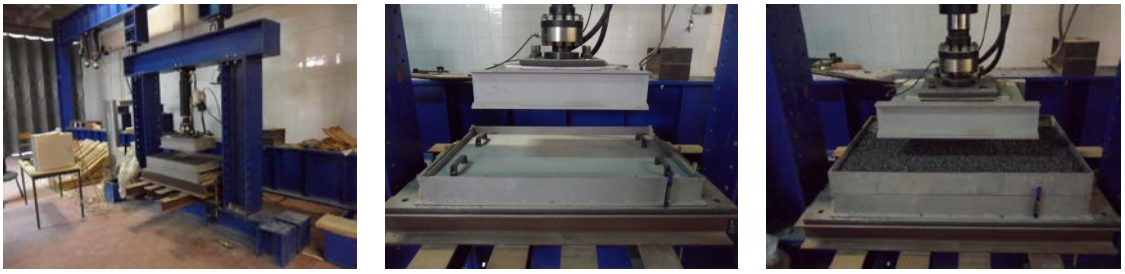

a) b) c)

Figure 3 – Laboratory mechanical damage tests: a) overview of the equipment; b) compaction of the first layer of aggregate; c) container ready for testing.

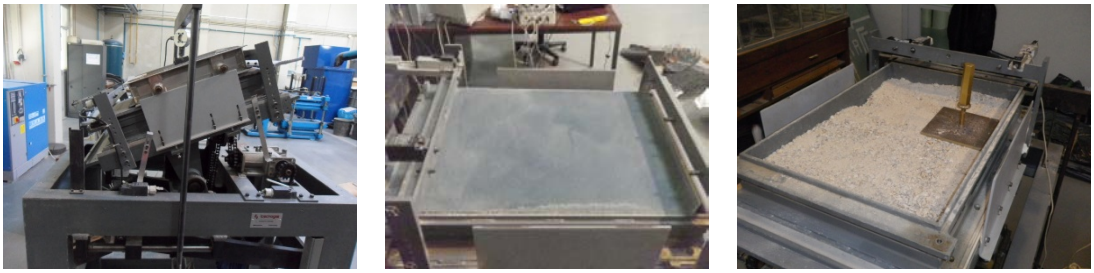

a) b) c)

Figure 4 – Inclined plane shear test equipment: a) during a test (upper box and geosynthetic supported on a rigid base); b) rigid base; c) lower box being filled with soil.

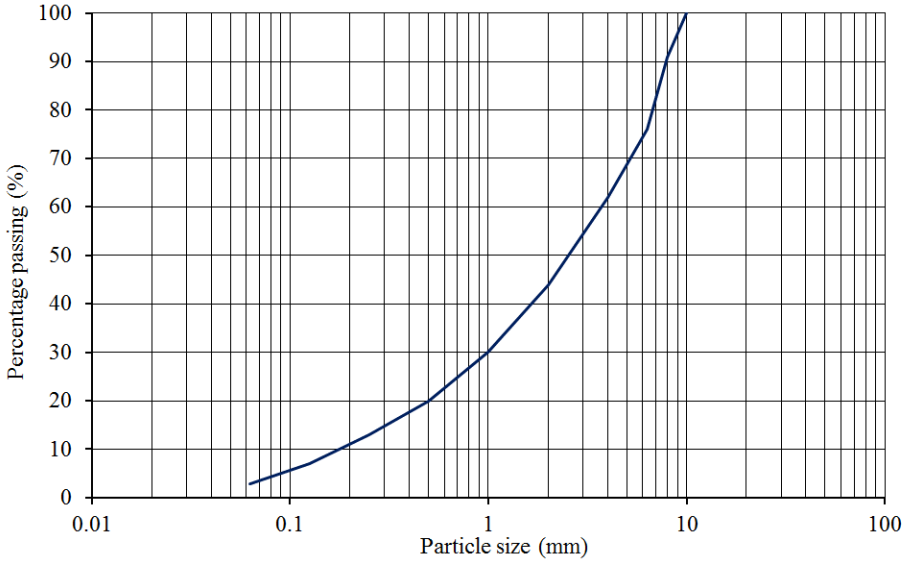

Figure 5. Particle size distribution of the soil used in the inclined plane shear tests.

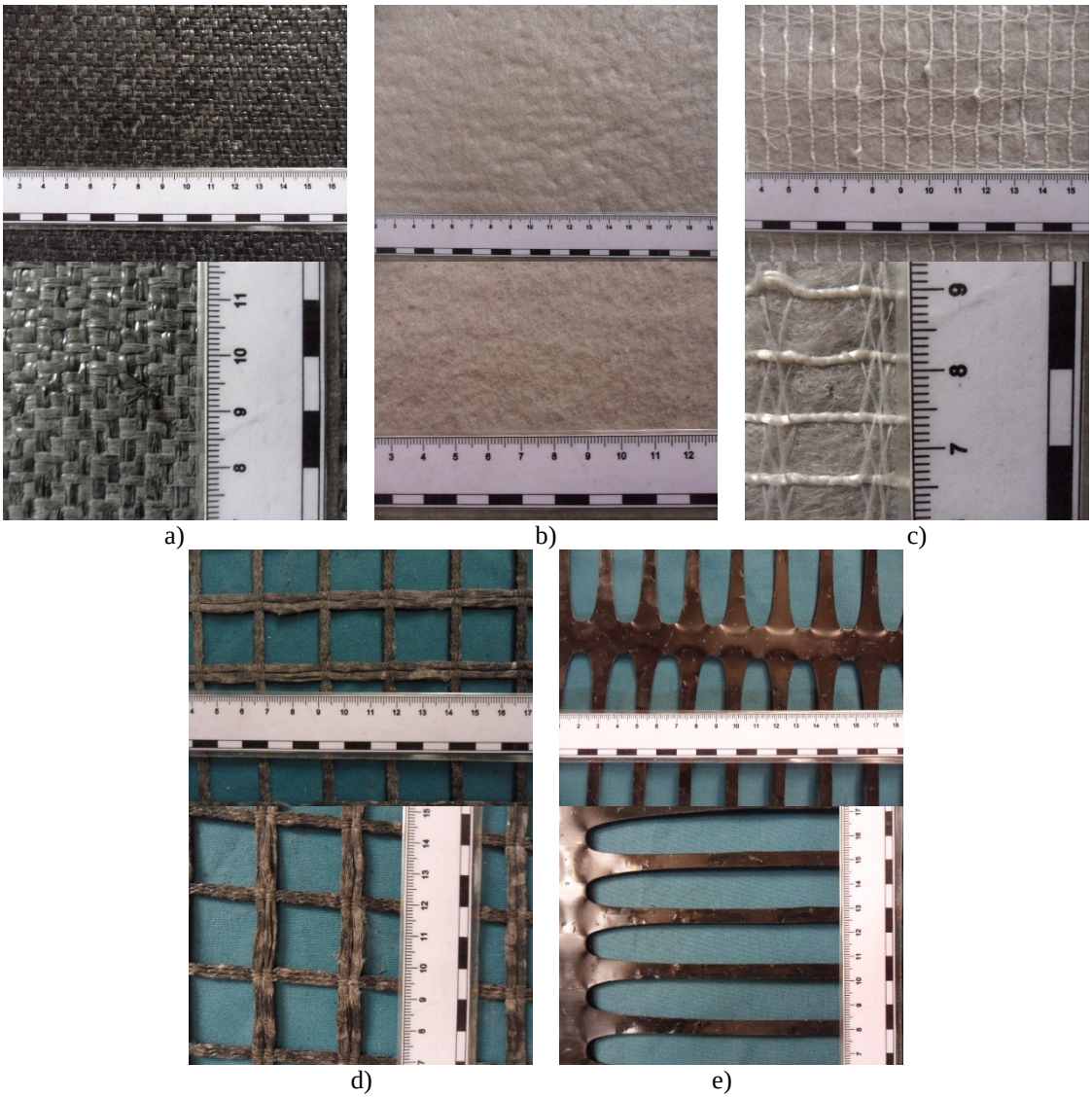

Figure 6. Examples of the visual inspection of specimens submitted to laboratory mechanical damage (LAB D): a) GTXw; b) GTXn; c) GCR; d) GGRw; e) GGRu.

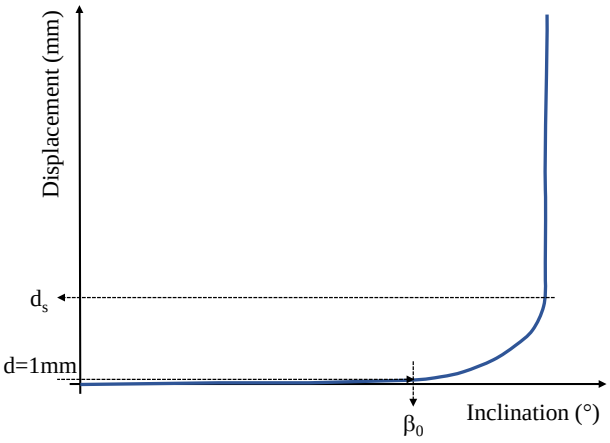

Figure 7. Criteria used to estimate parameters β_0 and d_S from the inclined plane shear tests results.

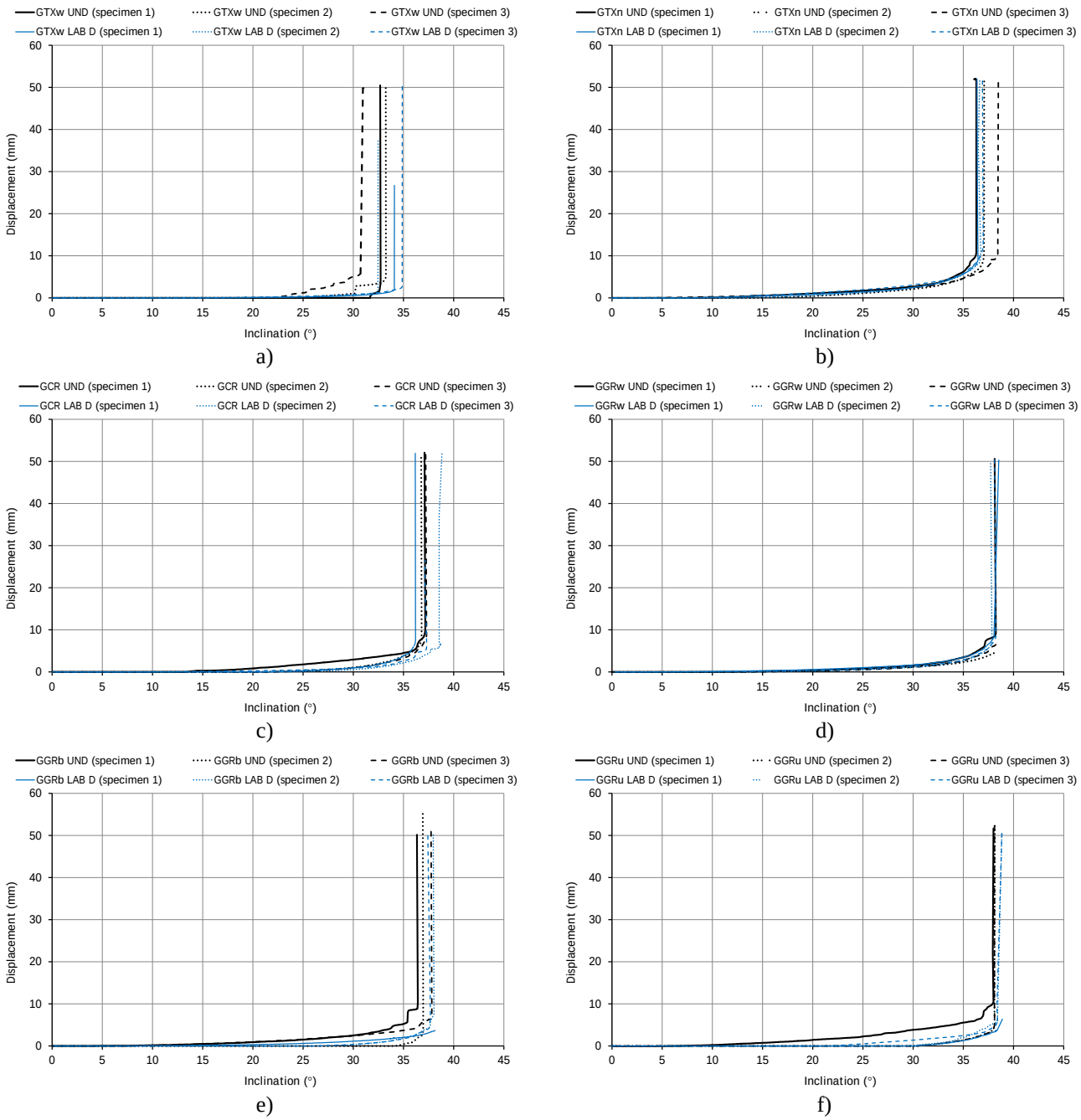

Figure 8. Inclined-shear plane response (displacement versus inclination curves) confined in soil (undamaged and after laboratory mechanical damage) for: a) GTXw; b) GTXn; c) GCR; d) GGRw; e) GGRb; f) GGRu.

1